Supplementary Material to:

Connection between the Tropical Pacific and Indian Ocean and Temperature Anomaly across West Antarctic

Ping Zhang[1,2], Anmin Duan[3,1,2*]

[1] *State Key Laboratory of Numerical Modeling for Atmospheric Sciences and Geophysical Fluid Dynamics (LASG), Institute of Atmospheric Physics, Chinese Academy of Sciences, Beijing 100029, China.*

[2] *College of Earth Science, University of Chinese Academy of Sciences, Beijing, 100049, China.*

[3] *State Key Laboratory of Marine Environmental Science, College of Ocean and Earth Sciences, Xiamen University, Xiamen 361102, China.*

**Corresponding author*: Anmin Duan, amduan@lasg.iap.ac.cn

Contents of this file：

Supplementary Figures 1 to 5

Supplementary Tables 1 to 2

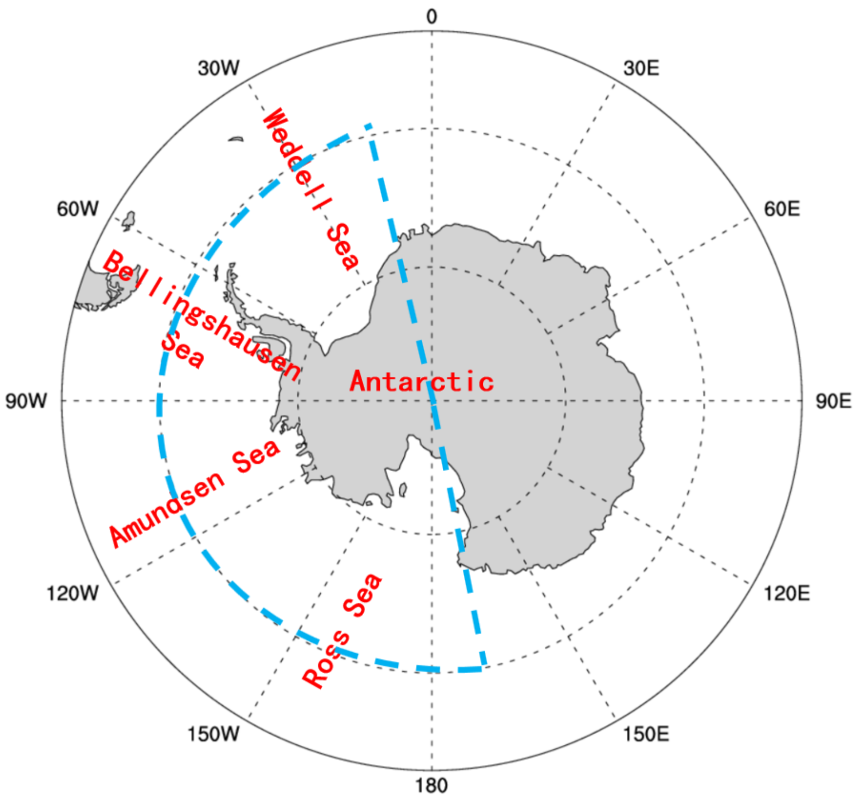

Supplementary Figure 1. Map of Antarctic. The region circled by the dashed blue line represents the West Antarctic (60°–90°S, 170°E–10°W), which is the target region in this study.

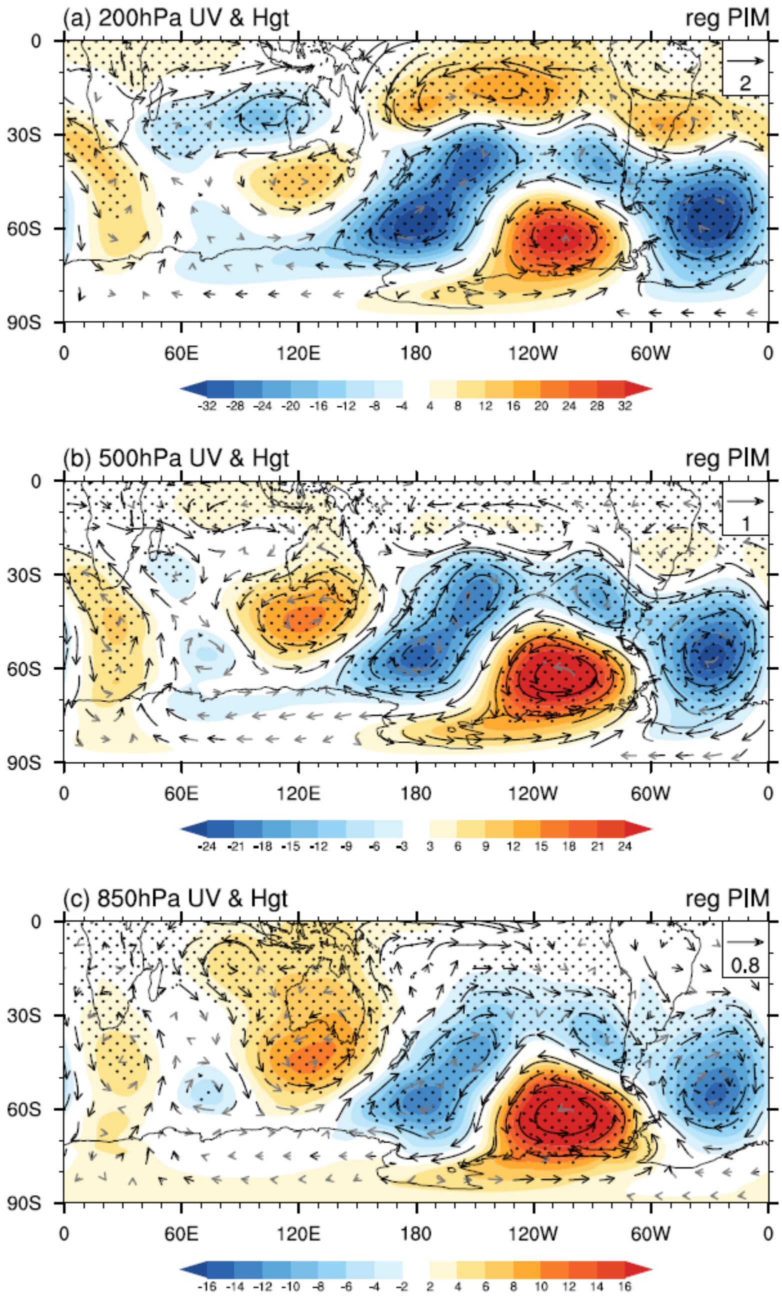

Supplementary Figure 2. Regression of anomalous circulation onto the PIM index in austral spring. (a) 200-hPa, (b)500-hPa, (c) 850-hPa geopotential height (shading; units: gpm), along with horizontal wind anomalies (vectors, units: m s^{-1}). The black vectors and stippled regions indicate statistical significance above the 95% confidence level.

During the positive phase of PIM, the 200hPa geopotential height displays two branches of poleward-arching wave trains, emitting from the tropical central-eastern Pacific and southeastern Indian Ocean, respectively. The two wave trains are featured by approximately equivalent barotropic structure in the extratropic but the baroclinic structure in tropics, with the low-level anticyclonic (cyclonic) anomaly and the upper-level cyclonic (anticyclonic) anomaly in the tropical southeastern Indian Ocean (central-eastern Pacific). This is indicative of a classic stationary Rossby wave response to tropical SST forcing.

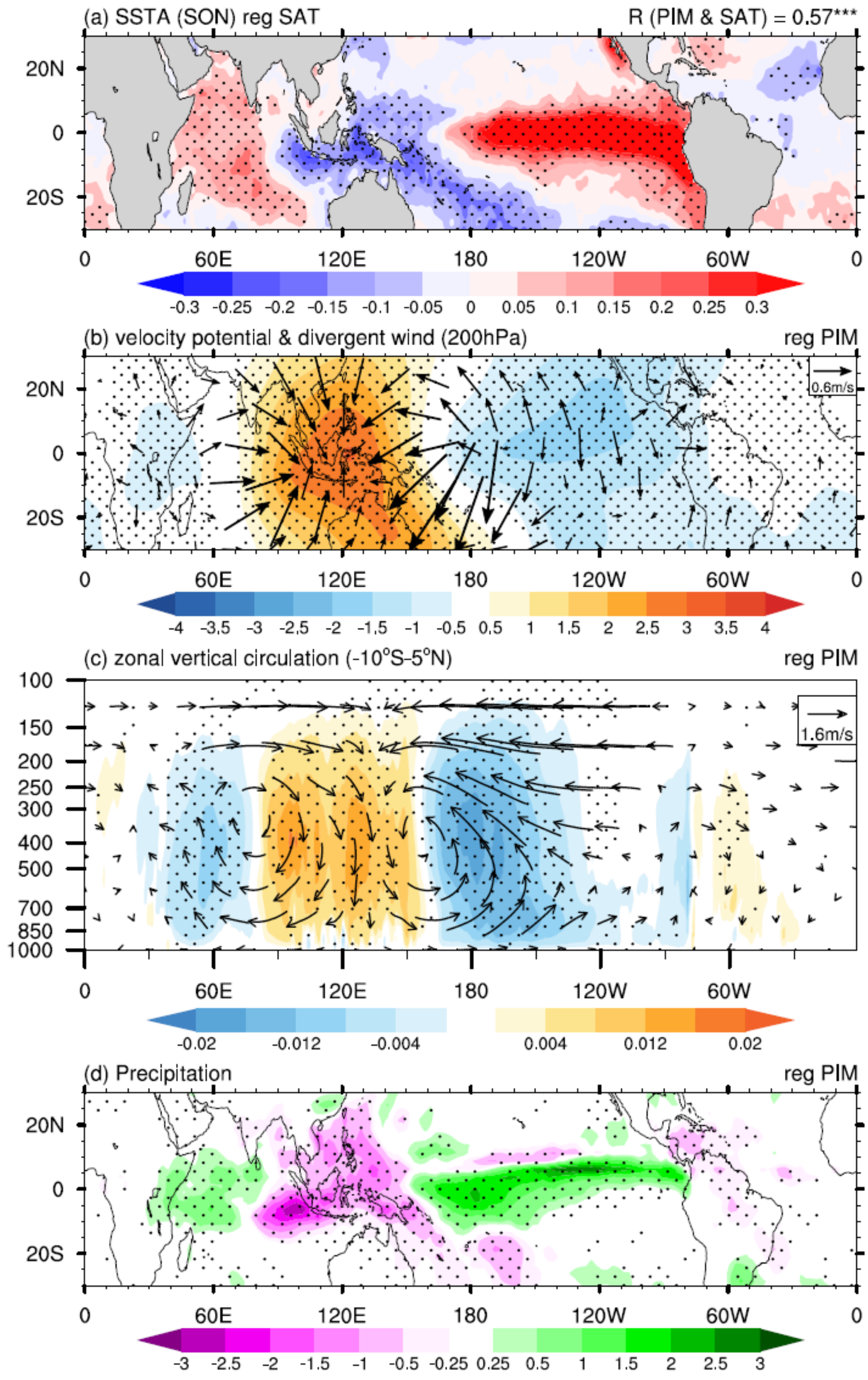

Supplementary Figure 3. Regression fields onto the PIM index in austral spring. (a) SSTA. (b) 200-hPa divergent wind field (vectors; units: m s^{-1}) and velocity potential field (shading; units: 10^6 m^2 s^{-1}). (c) Vertical velocity (shading; units: m s^{-1}) and zonal vertical circulation (vectors; units: m s^{-1}; vertical speed is scaled by 100 to facilitate visualization) averaged between 10°S and 5°N. (d) Precipitation (shading; units: mm day^{-1}). The black vectors and stippled regions indicate statistical significance above the 95% confidence level.

When the PIM is in the positive phase (Supplementary Figure 3a), in the upper level, there is a large-scale anomalous divergence (convergence) over the tropical central-eastern Pacific and western Indian Ocean (Maritime Continent) (Supplementary Figure 3b), which are reversed in the lower level (figure omitted). This results in the anomalous ascending motion and enhanced convection over the tropical central Pacific and western Indian Ocean, in contrast, an anomalous descending motion and suppressed convection around the Maritime Continent (Supplementary Figure 3c, S3d). The zonal gradients of the velocity potential near the equator are associated with the Walker circulation anomaly. That is, the PIM induces a tripole-like convection anomalies through exciting an anomalous “double-loop” Walker circulation in the tropical Pacific and Indian oceans. Subsequently, the associated convective heating acts as Rossby wave source to excite the stationary Rossby trains.

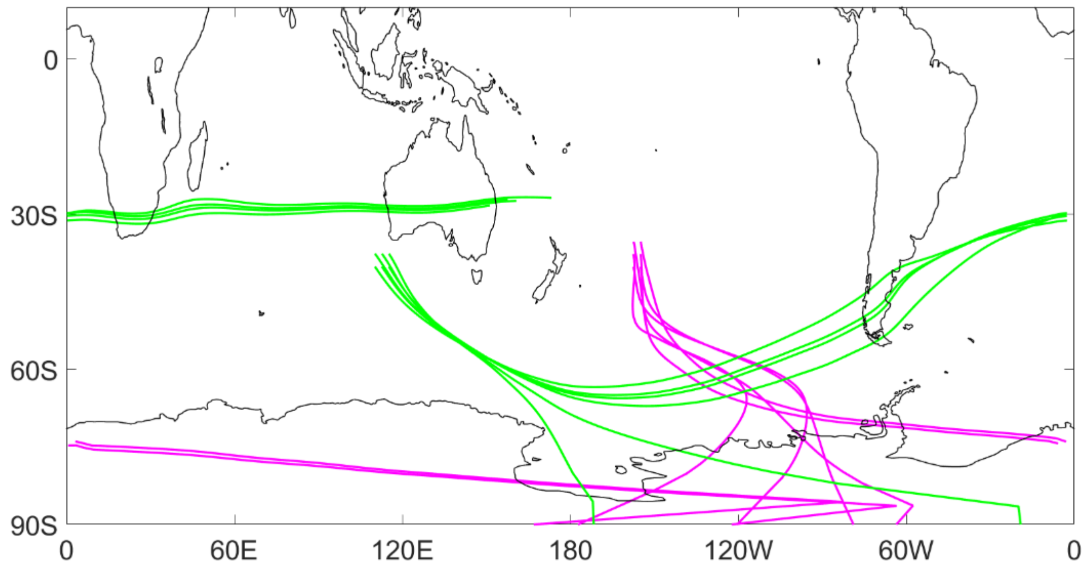

Supplementary Figure 4. Stationary Rossby wave trajectories with initial zonal wavenumber of k = 2 launched from the CEP (magenta lines) and MC (green lines). The climatological SON 200-hPa zonal winds are used as background flow. We initiate the wave trajectories from multiple launch points within a small area. Trajectories based on wavenumber k = 3 showed similar ray paths (omitted), but the wavenumber-2 scenario dominated more ray traces reaching into the West Antarctic.

Following Hoskins and Karoly (1981) and Li et al. (2015a), we calculate the Rossby wave ray tracing to further trace the propagation pathway of wave energy. Figure S4 depicts representative wave rays originating from the MC and CEP wave source regions with the initial wavenumber of k = 2 (details of calculation given in the caption). As shown in Supplementary Figure 4, both the wave rays originating from the CEP and MC regions traveled south poleward and then eastward, meeting together over the West Antarctica area. In addition, several ray traces from MC region keep propagate eastward along the subtropical jet. That is, most of these ray paths originating from the two regions closely resemble the arching wave patterns shown in observations (Fig. 2a, Fig. 2d) and AGCM simulations (Fig. 3c). The coherency between the observations, AGCM sensitivity experiments, and the Rossby wave ray tracing further verify the reliability and robustness of our conclusion.

Supplementary References:

Hoskins, B. J., & Karoly, D. J. The steady linear response of a spherical atmosphere to thermal and orographic forcing. J.Atmos. Sci., 38, 1175–1196 (1981).

Li, X., Gerber, E. P., Holland, D. M., & Yoo, C. A Rossby Wave Bridge from the Tropical Atlantic to West Antarctica. J. Climate, 28, 2256-2273 (2015a).

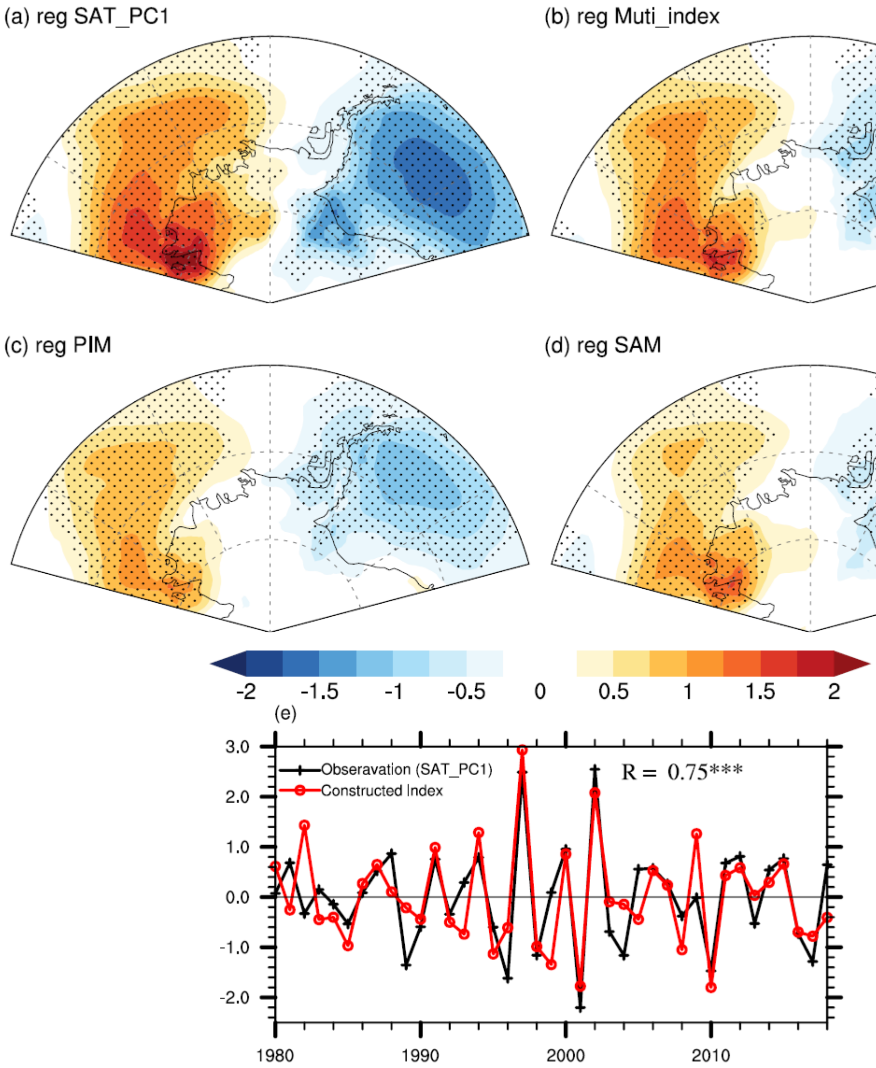

Supplementary Figure 5. Regression of SAT anomalies across West Antarctic onto the (a) SAT index, (b) constructed multiple regression index using the PIM and SAM index, (c) PIM index, and (d) Southern Annular Mode (SAM) index (multiply by -1) in austral spring. Stippled regions indicate statistical significance above the 95% confidence level. (e) The normalized time series of the dipole SAT anomalies across West Antarctic from observation (black line with crosses circles), hindcast (red line with open circles). The correlation coefficient between the observation and hindcast is shown in the upper-right corner of (e). *** represents the significance exceeding 99%

confidence level.

We found that, in addition to the PIM, there is also a robust correlation between SAM and the dipole SAT anomalies, with their correlation coefficient of -0.57 (Table S2). And the PIM and SAM are independent of each other. These motivate us to construct a multiple regression model using both the PIM and SAM indices, to improve the simulation of the SAT anomalies. The constructed index almost exactly matches with the observed dipole SAT index (Supplementary Figure 5e), with their correlation coefficient reaches 0.75 (> 99.9% confidence level), explaining nearly 57% of the variance of West Antarctic SAT (Table. S2). In addition, compared with the regression onto the PIM index (Supplementary Figure 5c) and SAM index (Supplementary Figure 5d), the West Antarctic SAT anomalies hindcast by the multiple regression model (Supplementary Figure 5b) almost exactly consistent with that in observation (Supplementary Figure 5a), both in the pattern and magnitude. These indicate the necessity of considering both factors to improve the accuracy of the simulation and prediction for West Antarctic SAT. Currently, this work only explored the PIM-induced effects. The physical mechanism of SAM affecting West Antarctic SAT and the combined effects induced by PIM-SAM together will be examined in another future work.

Supplementary Table 1. Designs of the AGCM experiments.

Experiment	Design
CTRL	Atmosphere forced by the climatological annual cycle of SST, with external forcing fixed at the year-2000 level. Integrated for 40 years, with the first 8 years used as spin-up.
PIM	Both the positive and negative anomaly experiments are integrated from May 1 to November 1, with the SST forcing in the tropical Pacific and Indian Ocean (20°S–20°N, 40°–80°W) restored to the model climatology plus the composite SSTA in the positive and negative PIM years [the PIM index greater (less) than +(−)1.0 standard deviation], respectively, from July to November. The ensemble consists of 32 members, which is restarted with different initial conditions provided by the outputs of CTRL run.
CEP	As in the PIM experiment, but with only the SST forcing in the tropical central-eastern Pacific (CEP).
MC	As in the PIM experiment, but with only the SST forcing in the Maritime Continent (MC).
CEP+MC	As in the PIM experiment, but with the combined SST forcing in the tropical central-eastern Pacific and Maritime Continent (CEP+MC).
WIO+MC	As in the PIM experiment, but with the combined SST forcing in the tropical western Indian Ocean and Maritime Continent (WIO+MC).

Supplementary Table 2. Correlation coefficients between the observed SAT index with the PIM, SAM, and the reconstructed indices in austral spring during 1980-2018, along with their explained variances for West Antarctic SAT anomalies. *** Coefficient exceeding the 99% confidence level. Note: the I_{PIM}, I_{SAM} and I_{SAT} indices are normalized time series.

	I_{PIM}	I_{SAM}	$I_{\mathrm{SAT}} = 0.498 \cdot I_{\mathrm{PIM}} - 0.501 \cdot I_{\mathrm{SAM}}$
Correlation with SAT (observation)	0.568***	0.570**	0.754***
Explained variance	32.2%	32.5%	56.9%